Program Digest, 2019 IEEE International Ultrasonics Symposium (IUS)
Glasgow, Scotland, October 6-9, 2019

Construction of FDMAS in Baseband and Its Performance Evaluation

Ryoya Kozai
Dept. of Electrical Engineering and Computer Science
Tokyo Metropolitan University
Tokyo, Japan
kouzai-ryouya@ed.tmu.ac.jp

Kan Okubo
Dept. of Electrical Engineering and Computer Science
Tokyo Metropolitan University
Tokyo, Japan
kanne@tmu.ac.jp

Norio Tagawa
Dept. of Electrical Engineering and Computer Science
Tokyo Metropolitan University
Tokyo, Japan
tagawa@tmu.ac.jp

Takasuke Irie
Dept. of Research and Development
Microsonic Co., Ltd
Dept. of Electrical Engineering and Computer Science
Tokyo Metropolitan University
Tokyo, Japan
irie@microsonic.co.jp

Masasumi Yoshizawa
Dept. of Monozukuri
Tokyo Metropolitan College of Industrial Technology
Tokyo, Japan
yoshizawa@metro-cit.ac.jp

***Abstract*— FDMAS (Filtered-Delay Multiply and Sum) has attracted attention in recent years as a receiving beamforming method with high lateral resolution. Since the FDMAS is processing in the RF (Radio Frequency) band, in order to reduce the sampling rate and the amount of memory required, realization in the baseband is desirable. On the other hand, we have proposed the super resolution method (SCM: Super-resolution FM-Chirp correlation Method) in the range direction as baseband processing. By integrating this with the FDMAS, we can expect super resolution in both the range and lateral directions. Considering processing transparency, it is desirable to extend the FDMAS to baseband processing. In this study, both methods are integrated by using the result of the SCM as the weight of the FDMAS beamforming, and its performance is evaluated.**

***Keywords*— FDMAS, super-resolution, frequency sweep transmission, MUSIC algorithm, baseband processing**

I. Introduction

Recent researches on ultrasonic beamforming methods has made particular progress in improving lateral resolution. The beamforming method is the basis of array signal processing using an array transducer composed of multiple transducer elements, and is a technology that generates spatial resolution by forming the directivity of the beam. The most basic beamforming method is DAS (Delay and Sum) [1], which equalizes the received signal delay of each element and then adds them. However, this technique is strongly limited by the beam width determined by the aperture width of the transducer array. In order to form a narrower beam, various beamforming have been proposed [2–4]. Recently, FDMAS (Filtered-Delay Multiply and Sum) beamforming [5], which can achieve high resolution and contrast without complicated calculations by using an approximate calculation of correlation between received signals of each element, has attracted attention. Various extensions of the FDMAS have been proposed in [6, 7]. On the other hand, we proposed methods for baseband processing called the SCM (Super-resolution FM-Chirp correlation Method) [8] and the SA-SCM (Synthetic Aperture-SCM) [9] to improve the range resolution. These methods realize super resolution in the range direction by using the phase information of the carrier wave by transmitting and receiving multiple pulses with different carrier frequencies. The SCM uses focused pulse transmission, and the SA-SCM is an extension of the SCM that uses divergent pulse transmission to increase the frame rate. The SA-SCM first applies receive beamforming [10] such as the DAS to echoes received by all elements. After calculating each line signal composing the image, the resolution is improved by applying the SCM. Since the SCM is a processing for each image line, discontinuity tends to occur in the lateral direction. To solve this problem, first, the SCM is applied to the received echo of each element, and the received echo is multiplied by the SCM result, and then the DAS is performed to generate a line signal with high range resolution. This method is called SCM-weighted SA, in which no lateral discontinuity occurs [11].

The FDMAS is processed in the RF (Radio Frequency) band and utilizes echo correlation calculations between elements to improve lateral resolution. As a result, a signal having twice the bandwidth appears in the second harmonic band of the fundamental frequency, which improves the resolution in the distance direction. Therefore, in order to reduce the sampling rate and the amount of memory required, it is desirable to implement in baseband. On the other hand, by adopting FDMAS as the receive beamformer used in SCM-weighted SA, higher resolution can be expected. Therefore, in this study, we first extend FDMAS to baseband processing. In order to integrate the SCM and the FDMAS, it is natural to realize the FDMAS in the baseband in terms of transparency, that is, computational efficiency. Therefore, in this study, the FDMAS is first constructed as a baseband processing. Then, we propose an integrated method that adopts the FDMAS as a receive beamformer in the SCM-weighted SA. According to this method, the lateral resolution of the conventional SCM-weighted SA can be improved and the resolution in the range direction can also be improved. The performance is confirmed by experiment.

II. Method

A. Super-resolution FM-Chirp correlation Method

The SCM improves the resolution in the range direction based on extraction of the signal subspace like as the MUSIC algorithm [12, 13]. To avoid echoes from different scatterers having coherence, an FM chirp signal is transmitted multiple times with different carrier frequencies. As a result, the signal subspace dimension corresponding to the number of scatterers present in each image line can be ensured.

To use the SCM results as a receive beamforming apodization in the same way as the SCM-weighted SA, the transmit position of multiple transmissions must be fixed at the same position on the array transducer. If the transmission of different frequencies is performed from different positions, the time position of the corresponding reflected waves cannot be aligned between echoes used for the SCM processing, and hence, the SCM processing cannot be performed correctly. This restriction is not a problem for phased array transducers. However, for linear and convex arrays, this restriction is not desirable for properly measuring information across the entire image area. Therefore, it is effective to perform transmission and reception multiple times at each position while changing the transmission position, but the necessary measurement time increases. In order to avoid this difficulty, it is effective to reduce the transmission position by applying a method based on the compressed sensing concept of [14].

B. Filtered-Delay Multiply and Sum in baseband

Like the DAS, the FDMAS corrects the delay time of the echoes received by many transducer elements. Baseband processing also requires phase correction because the phase is changed by correcting the delay time. In addition, because FDMAS processing performs multiplication between elements, the amplitude is scaled by taking the square root in advance. The received echo after correction is

$$s_{\mathrm{n}} = \sqrt{a_n} e^{j\theta_n}, \tag{1}$$

where s_n is the corrected IQ signal received by nth element, a_n is the amplitude of it and θ_n is its phase after phase correction. In the DAS, corrected echoes are added up, but in the FDMAS, the corrected echoes are multiplied by all pair combinations and added together. Assuming that the number of the received echoes is N, the number of all combinations of pairs is

$$\binom{N}{2} = \frac{N^2 - N}{2}. \tag{2}$$

The FDMAS multiplication processing is complex conjugate multiplication in baseband processing. That is

$$\hat{s}_{ij} = s_i s_j^H + s_j\, s_i^H, \tag{3}$$

where H indicates Hermitian transpose. From these equations, the signal after addition is

$$y_{\mathrm{FDMAS}} = \sum_{i=1}^{N-1} \sum_{j=i+1}^{N} \hat{s}_{ij} = \sum_{n=1}^{(N^2-N)/2} \hat{s}_n\,. \tag{4}$$

It is necessary to extract twice the frequency band using band-pass filter in the FDMAS in the RF band. On the other hand, the proposed baseband FDMAS does not require this filtering. In [15], baseband processing is performed for low-cost FDMAS processing. The difference between this method and our baseband FDMAS is the presence or absence of the square term of the received echo itself. Since we were studying baseband FDMAS independently of [15], we decided to propose a method different from [15]. From the viewpoint of computational complexity, the method of [15] is more effective.

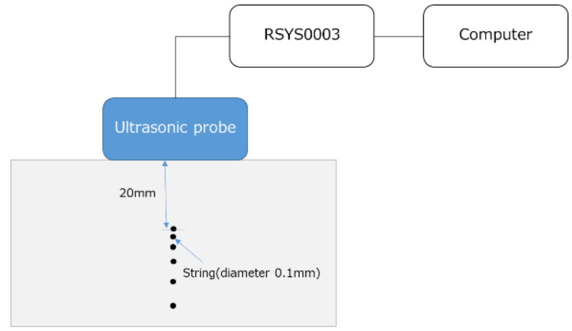

Fig. 1. Experimental setting for soft tissue-mimicking phantom.

TABLE I. PARAMETER SETTINGS OF THE TRANSMITTED FM-CHIRP PULSE

Parameter	Value
Frequency band width	2MHz
Chirp pulse duration	5μs
Variation range of center freq.	5 to 9 MHz
Number of transmission	30
Apodization	Hanning window

In this study, the SCM is applied to the IQ echo received by each element, and the target signal in IQ echo is thinned by applying the SCM result to the IQ echo as an apodization function, and then beamforming is performed by the FDMAS. We call this method HRR-FDMAS (High Range Resolution-FDMAS).

III. RESULTS

A. Experiment conditions

In the experiments, the transmission and reception sequences were generated using an experimental platform for medical ultrasound (RSYS0003, Microsonic Inc., Japan) with a sampling rate of 31.25 MHz. The number of transducer elements used for both transmission and reception is 64, while the element pitch is 0.315 mm. Transmitted waves are restricted to 7-level quantization. A linear array probe (T0-1599, Nihon Dempa Kogyo Co., Ltd., Japan) was also used. This probe's center frequency is 7.5 MHz and its specific bandwidth is 70%. The signal processing was performed offline using MATLAB software.

B. Experiment using soft tissue-mimicking phantom

Fig. 1 shows the experiment setting. We present the experimental results obtained using a soft tissue-mimicking phantom (US-2 multi-purpose phantom N-365; Kyoto Kagaku Co., Ltd., Japan), with a speed of sound of 1,432 m/s (25°C) and attenuation of 0.59 dB/cm/MHz. As shown in Fig. 1, the phantom includes six string wires, each of which has a diameter of 0.1 mm. The distances between these wires are 1.0 mm, 2.0 mm, 3.0 mm, 4.0 mm and 5.0 mm, measured from the side closest to the phantoms surface. Plane waves with amplitude value set to 45 V was transmitted using 64 elements. The phantom temperature was 26 ℃ at the time of measurement.

Because the probe element spacing is wider, it is likely that grating lobes will be formed. The frequency band of the FM chirp pulse that is used in the experiment is set at a relatively narrow 2 MHz, as described in the Table I. Although the frequency band that is used is not the most effective band for all the transmissions, it was confirmed that can be performed appropriately.

C. *Experimental performance evaluation*

First, we compare the FDMAS in the RF band and the FDMAS in the baseband. Fig. 2 shows the intensity distribution profile after beamforming on a line across the foremost target. Since the reception echoes of multiple frequencies are obtained for the SCM processing, it is possible to generate a B-mode image using each frequency echo. In this study, the lowest frequency of 5.5 MHz was used for imaging to avoid grating lobes as much as possible. Fig. 2 shows that the FDMAS does not change the range resolution compared to the DAS, but improves lateral resolution. Although, the amplitude bias is observed in the region where no signal exists in the FDMAS in the baseband. We think this is because the proposed FDMAS in the baseband obtains the correlation value by complex conjugate, so cancellation at a position where there is no signal does not work very much.

Next, performance of the HRR-FDMAS is evaluated. Fig. 3 shows the B-mode images, and Fig. 4 shows the intensity distribution profiles on a line crossing the foremost target by all methods considered. Table II shows range and lateral resolution at the foremost target. In this experiment, the signal subspace setting for the SCM processing was set to 4. From these results, it can be confirmed that the two methods using the SCM have significantly improved range resolution. It can also be seen that the lateral resolution of the SCM-weighted SA is improved by using the results of the SCM as apodization. In addition, the lateral resolution of the HRR-FDMAS is further improved. Fig. 5 shows -6dB range width at the foremost target after the HRR-FDMAS processing when the number of frequency sweeps is changed. From this result, the range resolution improves as the number of frequency sweeps increases. This is because the signal subspace can be extracted better by increasing the number of frequency sweeps. Therefore, the SCM performance is significantly affected by the number of frequency sweeps.

IV. CONCLUSION

We first proposed the realization of the FDMAS in baseband. Subsequently, we proposed a new method HRR-FDMAS in which the SCM result is applied to the FDMAS in order to improve range resolution. The improvement of the spatial resolution for the FDMAS in the conventional RF band was clearly confirmed by experiments. Evaluation and verification of actual performance of the HRR-FDMAS for living organisms is a task to be carried out as soon as possible in the future. In the HRR-FDMAS, the SCM processing takes much computational cost because the phase information of the carrier is extracted by the MUSIC algorithm that requires the eigenvalue analysis. Therefore, we are considering improving the range resolution by other methods that can use phase information with a low cost procedure. The essence of the SCM is to transmit and receive multiple times while changing the carrier frequency irregularly, and we aim to propose an efficient beamforming method that can take advantage of this principle.

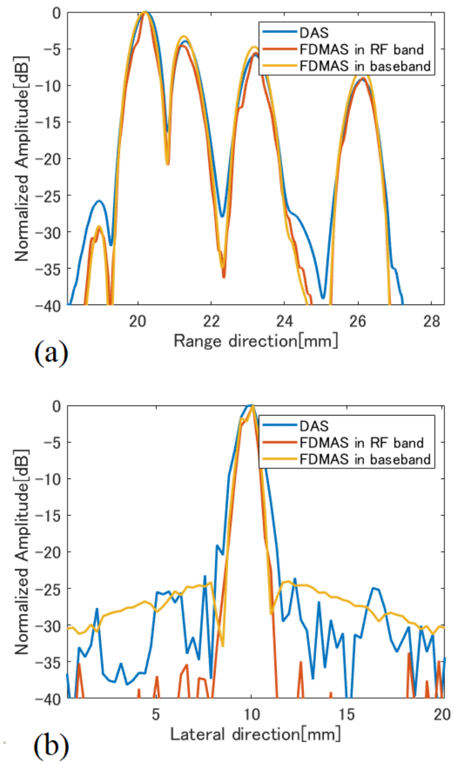

Fig. 2. Intensity distribution profiles after beamforming on a line crossing the foremost target: (a) range direction; (b) lateral direction.

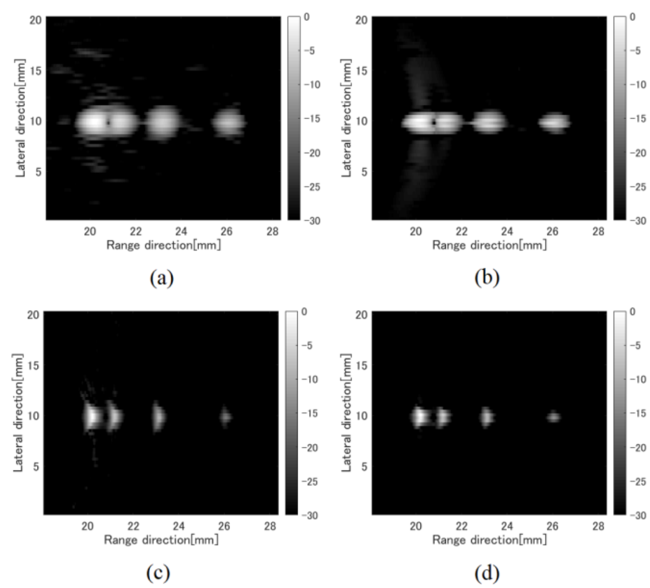

Fig. 3. B-mode images: (a) DAS; (b) FDMAS; (c) SCM-weightted SA; (d) HRR-FDMAS.

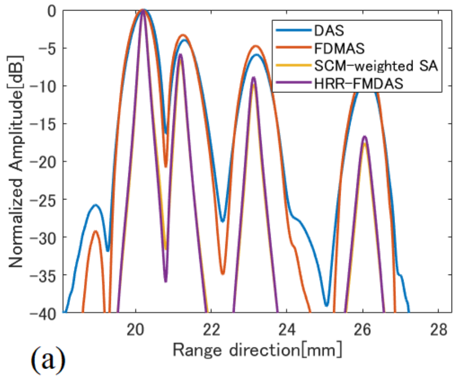

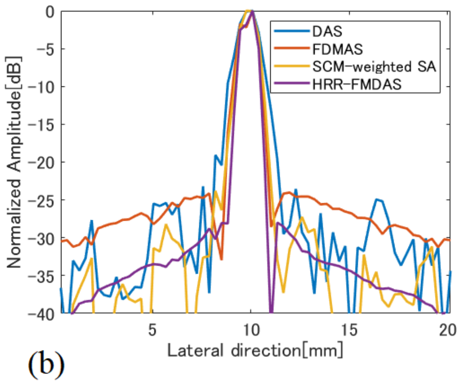

Fig. 4. Intensity distribution profiles on a line crossing foremost target in all the methods considered: (a) range direction; (b) lateral direction.

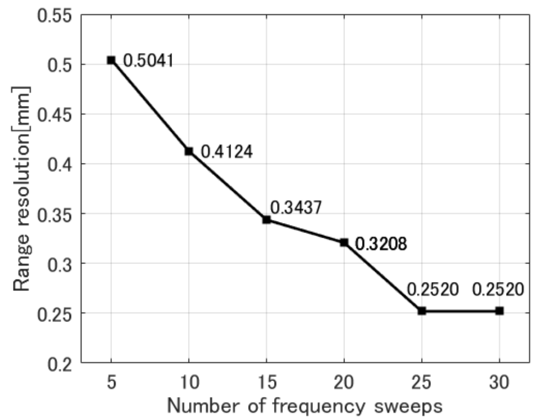

Fig. 5. -6dB range width at the foremost target after HRR-FDMAS processing when the number of frequency sweeps is changed.

TABLE II. RANGE AND LATERAL RESOLUTION AT THE FOREMOST TARGET

	Range width[mm]			Lateral width[mm]		
Method	-6dB	-10dB	-20dB	-6dB	-10dB	-20dB
DAS	0.82	1.03	2.61	1.26	2.21	2.84
FDMAS	0.8	0.99	1.35	1.26	1.58	2.21
SCM-weighted SA	0.25	0.37	0.71	1.26	1.26	2.21
HRR-FDMAS	0.25	0.37	0.69	1.26	1.26	1.56

REFERENCES

[1] K. E. Thomenius, "Evolution of ultrasound beamformers," In Proc. IEEE Int. Ultrason. Symp., vol. 2, 1996, pp. 1615–1622.

[2] Z. Wang, J. Li and R. Wu, "Time-delay and time-reversal-based robust capon beamformers for ultrasound imaging," IEEE Trans. Med. Imag., vol. 24, no. 10, pp.1308–1322, 2005.

[3] J. Camacho, M. Parrilla and C. Fritsch, "Phase coherence imaging," IEEE Trans. Ultrason., Ferroelectr., Freq. Control, vol. 56, no. 5, pp. 958–974, 2009.

[4] P. C. Li and M. L. Li, "Adaptive imaging using the generalized coherence factor," IEEE Trans. Ultrason. Ferroelectr. Freq. Control, vol. 50, no. 2, pp. 128–142, 2003.

[5] G. Matrone, S. A. Savoia, G. Caliano and G. Magenes, "The delay multiply and sum beamforming algorithm in ultrasound b-mode medical imaging," IEEE Trans. Med. Imag., vol. 34, no. 4, pp.940–949, 2015.

[6] G. Matrone, A. Ramalli, S. A. Savoia, P. Tortoli and G. Magenes, "High frame-rate, high resolution ultrasound imaging with multi-line transmission and filtered-delay multiply and sum beamforming," IEEE Trans. Med. Imag., vol. 36, no. 2, pp.478–486, 2017.

[7] G. Matrone, A. Ramalli, P. Tortoli and G. Magenes, "Experimental evaluation of ultrasound higherorder harmonic imaging with filtereddelay multiply and sum (f-dmas) non-linear beamforming," Ultrasonics, vol. 86, pp.59–68, 2018.

[8] M. Fujiwara, K. Okubo and N. Tagawa, "A novel technique for high resolution ultrasound imaging using super resolution fm-chirp correlation method (scm)," In Proc. IEEE Int. Ultrason. Symp., 2009, pp. 2390–2393.

[9] T. Wada, Y. Ho, K. Okubo and N. Tagawa, "High frame rate super resolution imaging based on ultrasound synthetic aperture scheme," Physics Procedia, vol. 70, pp.1216–1220, 2015.

[10] J. A. Jensen, S. I. Nikolov, K. L. Gammelmark and M. H. Pedersen, "Synthetic aperture ultrasound imaging," Ultrasonics, vol. 44, pp.e5–e15, 2006.

[11] J. Zhu and N. Tagawa, "Super-resolution ultrasound imaging based on the phase of the carrier wave without deterioration by grating lobes," In Proc. Int. Conf. Pattern Recognition, 2018, pp. 2791–2796.

[12] R. O. Schmids, "Multiple emitter location and signal parameter estimation," IEEE Trans. Antenas and Propagation, vol. 34, no. 3, pp.276–280, 1986.

[13] L. Zhou, Y. J. Zhao and H. Cui, "High resolution wideband doa estimation based on modified music algorithm," In Proc. IEEE Int. Conf. Inf. Automat, 2008, pp. 20–22.

[14] J. Liu, Q. He and J. Luo, "Compressed sensing based synthetic transmit aperture imaging: Validation in a convex array configuration," IEEE Trans. Ultrason. Ferroelectr. Freq. Control, vol. 65, no. 3, pp.300–315, 2018.

[15] C. C. Shen and P. Y. Hsieh, "Ultrasound baseband delay-multiply-and-sum (bb-dmas) nonlinear beamforming," Ultrasonics, vol. 96, pp.165–174, 2019.